



¹⁸F-FDG PET/CT: Brain Imaging

4

April-Louise Smith and Anna Barnes

Contents

4.1	Introduction.....	23
4.2	Patient Preparation.....	24
4.3	Imaging Protocol.....	24
4.4	Image Processing and Display.....	28
4.5	Quantification.....	30
4.5.1	Anatomical Standardisation.....	32
4.5.2	Intensity Normalisation.....	32
4.5.3	Statistical Analysis.....	33
4.5.4	Limitations.....	34
	References.....	35

4.1 Introduction

¹⁸F-2-Fluoro-2-deoxyglucose (¹⁸F-FDG) can be used to image regional cerebral glucose consumption which allows diagnostic imaging for a number of neurological indications such as dementia, epilepsy and movement disorders. Although not often used in neuro-oncology, it remains the method of choice in the diagnosis and staging of CNS lymphoma. Adhering to guidelines for patient preparation, using the correct imaging acquisition and reconstruction parameters, as well as defining the optimal image display for reporting are all crucial in order to obtain images of diagnostic quality. Furthermore, reporting images in the presence of neurological degenerative diseases can benefit hugely using additional

A.-L. Smith (✉) · A. Barnes
Institute of Nuclear Medicine, University College London Hospital NHS Foundation Trust,
London, UK
e-mail: april-louise.smith@nhs.net

post-processing and quantification of the images [1, 2]. This chapter summarises published guidelines, at the time of writing, on optimal imaging procedures for brain ^{18}F -FDG PET/CT and introduces the reader to some of the more widely available quantification tools and references for optional further reading of developments in the field.

4.2 Patient Preparation

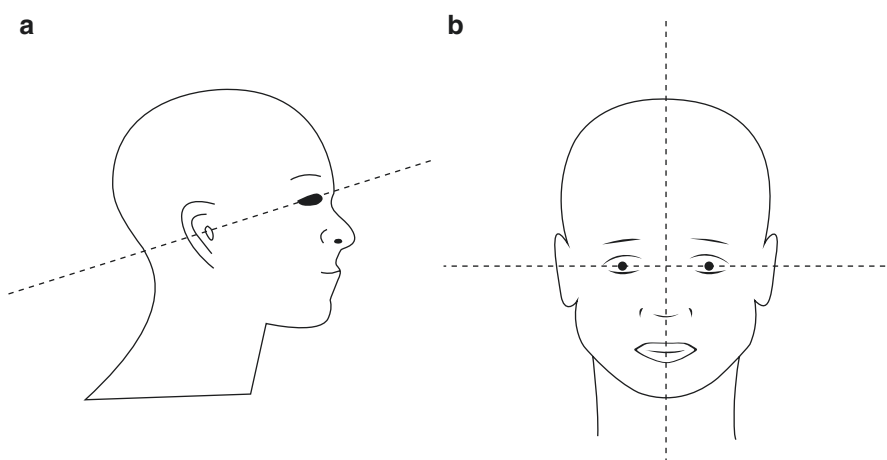
Patient preparation is broadly similar for all ^{18}F -FDG imaging studies; patients should fast prior to injection. European and American guidance advise 4–6 h [3, 4] to prevent competition between elevated plasma glucose and FDG, especially since the injected volume is at trace concentrations. For this reason it is also recommended that blood glucose levels are checked before administration; European and American guidelines state that patients should be rescheduled if glucose levels are >160 mg/dL [1] or >150 – 200 mg/dL [2], respectively, and also give recommendations for diabetic patients. Caffeine, alcohol or drugs that may affect cerebral glucose metabolism must also be avoided [5] during the fasting period. Patients are required to stay in a quiet and dimly lit room for several minutes prior to injection and during the uptake phase to avoid enhanced uptake due to brain activity [6] typically in the visual and/or auditory cortex. So for interictal epilepsy imaging, it is important to ensure the patient has not had a recent seizure and the activity is not administered unless the patient has been seizure-free for at least 20 min [3, 4] since for this test the associated affected cortex is detected as a region of hypo-glucose metabolism during the interictal state. There have been some studies that suggest the patient should be seizure-free for at least 24 h prior to imaging since glucose hypermetabolism after a partial seizure may not return to baseline immediately [5, 7]. In the clinical setting, this may not be feasible, but it remains essential that the reporting radiologist is aware of seizure activity that may have occurred prior to imaging. In fact both European and American guidelines suggest EEG monitoring for 2 h prior to injection could help in this regard.

4.3 Imaging Protocol

Table 4.1 outlines the recommended administered activity in the UK for ^{18}F -FDG brain imaging, and associated doses taken from the Administration of Radioactive Substances Advisory Committee (ARSAC) note for guidance [8]. Paediatric administered activity should be kept to a minimum but while still allowing for acceptable image quality. To ensure a robust signal, the reduced activity can be calculated using scaling factors for appropriate patient weights. ARSAC guidance supports advice on scaling provided by the European Association of Nuclear Medicine (EANM) [9] but are of the view that more research is required and further optimisation should be conducted locally. As with all PET/CT, imaging pregnancy is contraindicated.

Table 4.1 ARSAC guidance for administered activity and associated patient dose [8]

Investigation	Radionuclide	Chemical form	Diagnostic reference level (MBq)	Effective dose (mSv)	Dose to the uterus (mGy)
Brain tumour imaging	^{18}F	FDG	250	4.8	4.5
Differential diagnosis of dementia					
Focal epilepsy					

**Fig. 4.1** Patient positioning for brain imaging. (a) Orbital-meatal plane (b) Median sagittal plane

After the injection the patient should remain in a quiet darkened room for a minimum of 30 min [3], although a longer uptake time is useful for neuro-oncological applications since it can give better differentiation between tumour and normal brain tissue. In fact, a longer time of 60 min is usually used in clinical practice since this allows better contrast between white and grey matter in the cortex and still provides sufficient counts for acceptable image quality. It would be advisable, however, for the uptake time to be decided locally and standardised for repeatability; for example, in a busy nuclear medicine department, it is also easier to schedule alongside other FDG PET/CT imaging of the body which requires a minimum 60 min uptake for optimal imaging in oncology, and the ability to schedule PET/CT imaging efficiently should not be taken lightly.

Once sufficient uptake time has passed, the patient should be carefully positioned, aligning the orbital-meatal plane in the x -axis and median sagittal plane in the y -axis as demonstrated by the diagram in Fig. 4.1.

Modern PET scanners operate in 3D image acquisition mode (as opposed to 2D with collimation) which allows acceptable image quality with 50–200 million detected events [3]; this can equate to scanning times of 10–30 min depending on the scanner sensitivity. Reconstruction of PET images uses an iterative technique which combines information about the scatter properties of the radionuclide as well as the geometry of the scanner to improve image contrast and signal to noise ratio [10]. The last step to providing images for reporting by the radiologist is to apply attenuation correction to account for the attenuating properties of the tissue through which the photon passes. In order to apply this correction, an attenuation map is created using either a transmission scan (a photon source that rotates around the patients head before the scan) or for hybrid scanners, a low-resolution CT or MR image for PET/CT and PET/MRI, respectively. Figure 4.2a shows a uniform region of a phantom with no attenuation correction, giving the appearance of

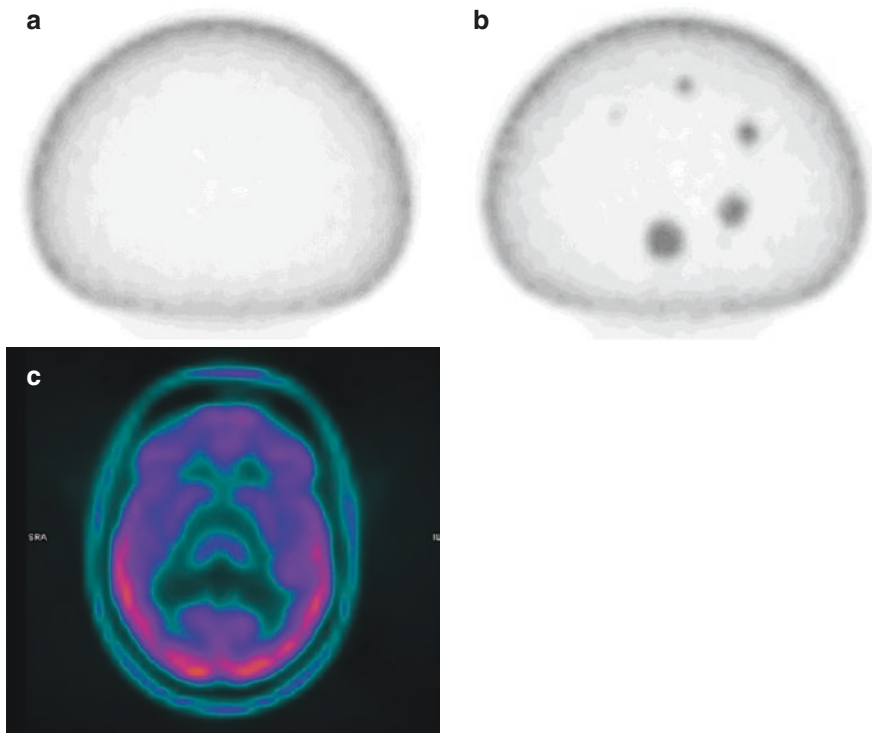


Fig. 4.2 Images with no attenuation correction. (a) Uniform area of phantom. (b) Active spheres in image quality phantom. (c) Example patient ^{18}F -FDG brain image

higher activity at the edge of the phantom. In Fig. 4.3a, the CT attenuation correction has corrected for the counts lost from the centre of the phantom, giving a more uniform appearance. The importance of this correction is further highlighted by Figs. 4.2b and 4.3b where you can see the spheres are clearer in the corrected image (Fig. 4.2b) with better image contrast. Figure 4.2c illustrates this effect on a brain image showing the reduction of detail seen compared to the attenuation corrected image (Fig. 4.3c). One of the recent developments in PET scanner technology is that of PET/MRI a hybrid scanner that is able to image using PET and MR simultaneously. Unlike x-ray CT, the intensity values within a MR image are not directly related to the attenuating properties of the tissue and so a pseudo-CT must be created by assigning a fixed CT value to certain categories of tissue, cortical bone, brain and air (see Fig. 4.4). However, imperfections in the complete

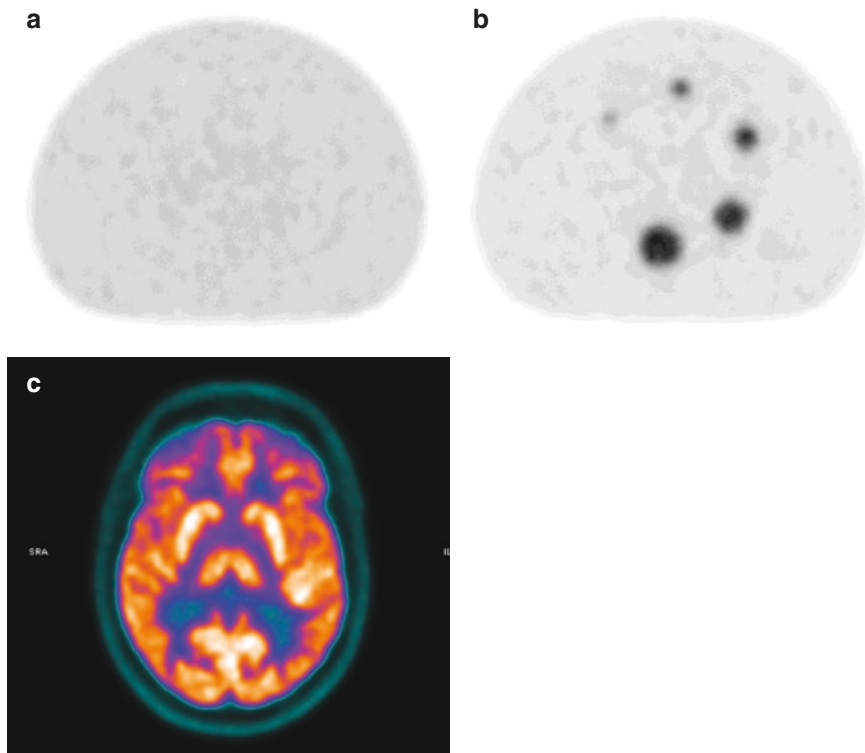


Fig. 4.3 Images with attenuation correction. (a) Uniform area of phantom. (b) Active spheres in image quality phantom. (c) Example patient ^{18}F -FDG brain image

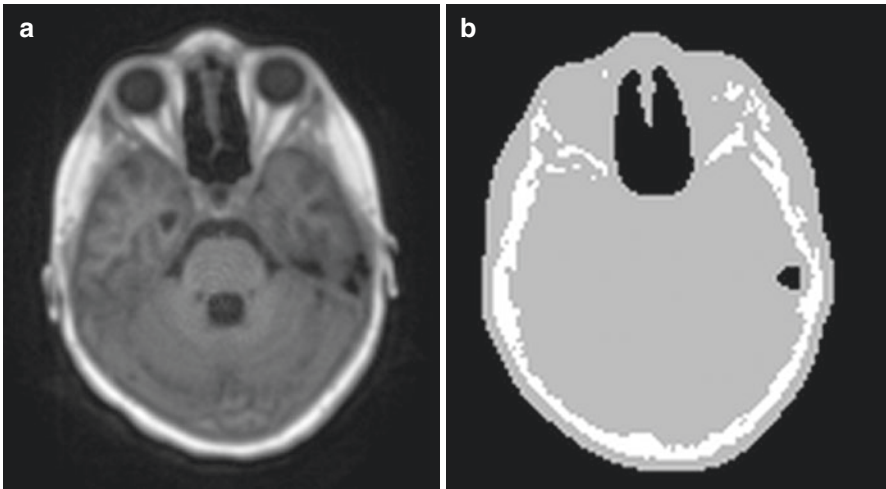


Fig. 4.4 PET/MR attenuation correction map. (a) MR UTE image used to create the μ -map. (b) MR μ -map showing the different categories (brain, bone and air) tissues has been assigned to

representation of cortical bone in the image can lead to discrepancies in tracer uptake values [11].

Image acquisition can take anywhere between 10 and 30 min, and therefore it is essential to ensure that steps are taken to prevent patient movement both during the acquisition and between the CTAC or MRAC and the PET. A radiographer/nuclear medicine technologist will clearly explain the procedure to the patient and the requirement to remain still. Once the patient has been placed in the preferred orientation (this may be harder in elderly patients due to limited flexibility), they should be restrained but made to feel comfortable by using padding or bandages to hold the head in place. Another measure that can be taken is to acquire the data dynamically (using list mode) and to allow the data to be checked for movement after acquisition (e.g. by reconstructing images at short frame durations), and then the final image is compiled from the frames unaffected by motion. Guidance on image reconstruction is provided by EANM [3].

4.4 Image Processing and Display

Once reconstructed, it is important to ensure that the images are correctly displayed in a standard anatomical position in order to ensure consistent reporting and avoid potential artefacts in the image (Fig. 4.5). This is particularly important in reporting of interictal epilepsy images where asymmetries in the uptake pattern in the temporal lobes are indicative of seizure focus. Although software can be used to align the images in post-processing, correct patient positioning helps this process. The images can also be co-registered with high-resolution x-ray CT or MR for structural

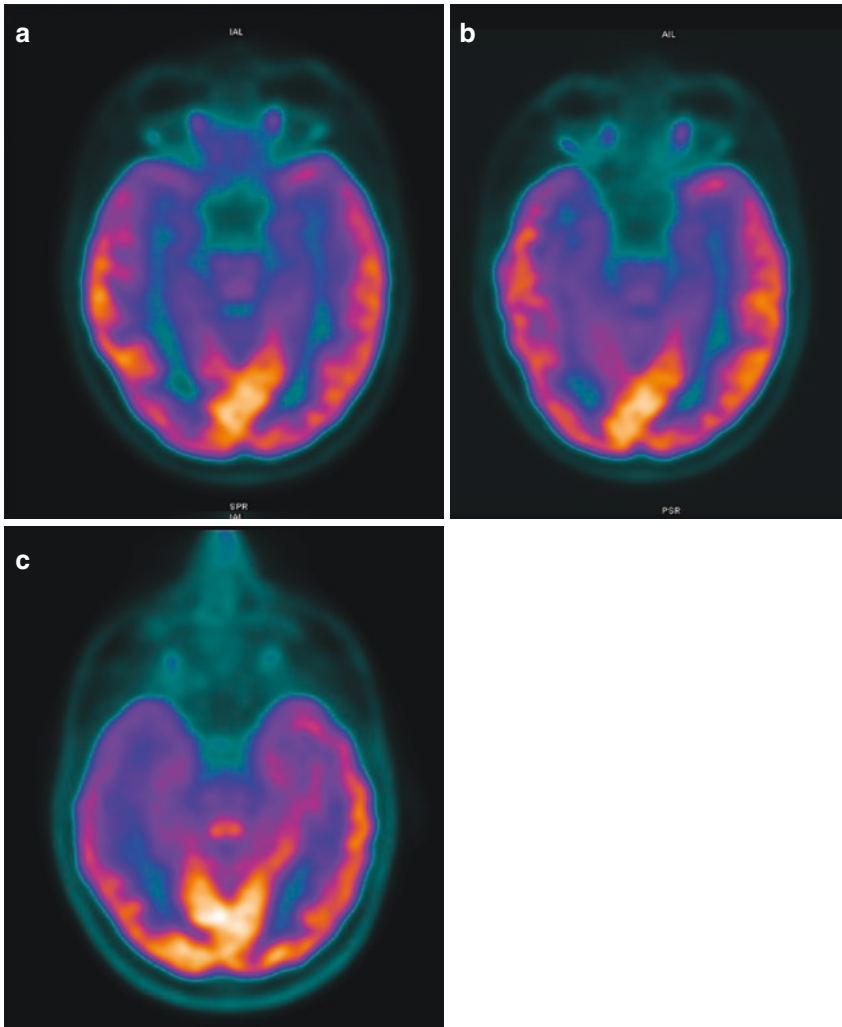


Fig. 4.5 An example of two ^{18}F -FDG brain PET/CT patient images with indication of epilepsy. The images show how misalignment can contribute to image artefacts. (a) Patient 1: A ^{18}F -FDG brain PET/CT epilepsy scan with normal uptake that has been correctly aligned. (b) Patient 1: The same patient with the images rotated in the coronal plane giving an impression of asymmetry in uptake and the potential to be incorrectly reported as the right temporal lobe epilepsy. (c) Patient 2: A correctly aligned patient with right temporal lobe epilepsy for comparison

comparisons and anatomical localisation. Images can be displayed in the transaxial, coronal and sagittal planes for reporting, as shown in Figs. 4.6 and 4.7. Further orientations can be used such as the long axis of the temporal lobes (Fig. 4.7c) to provide a more informative representation of the medial temporal lobe in the reporting of interictal images.

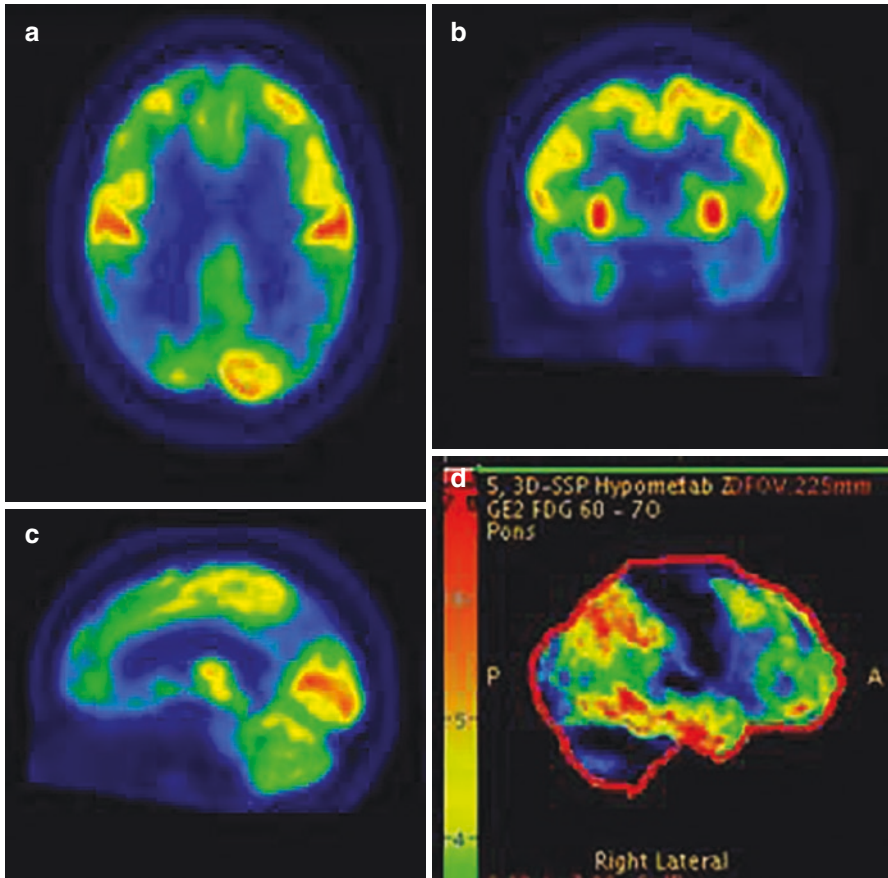


Fig. 4.6 ^{18}F -FDG brain PET/CT for dementia showing optimal display as well as 3D-SSP (stereotactic surface projections) with typical patterns of reduced uptake indicative of Alzheimer's disease. (a) Transaxial slice. (b) Coronal slice. (c) Sagittal slice. (d) 3D-SSP showing significant areas of reduced uptake (normalised to pons). Panel d demonstrates surface-rendered images of the statistical analysis. Showing a z -score map normalised using the pons with a threshold of $z > 2$

4.5 Quantification

There are a variety of PET analysis methods to quantify functional information related to neurodegenerative disease. There are several commercial software packages available (CortexID, GE; Scenium, Siemens; BRASS, Hermes; Vista, MIM and more); none are approved to be used without the supervision of a radiologist that provides this quantitative information to assist with the visual reporting of images. What all these software packages have in common is an image realignment

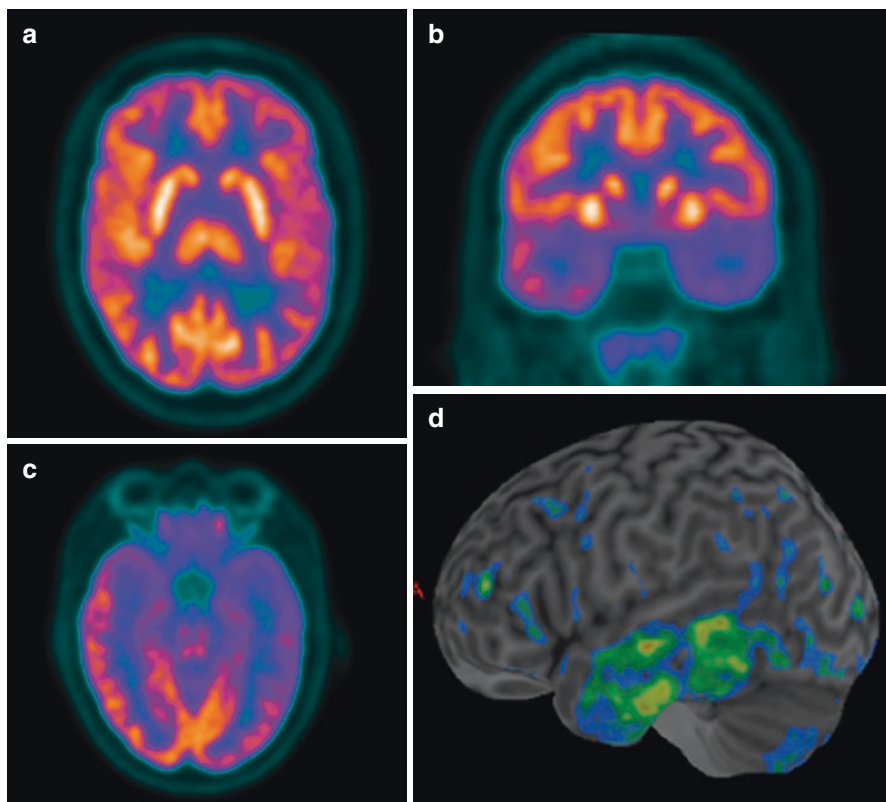
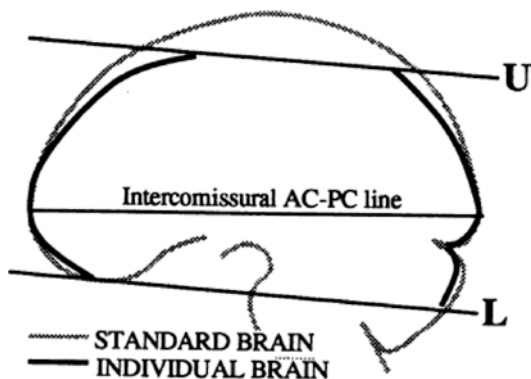


Fig. 4.7 ^{18}F -FDG brain PET/CT for epilepsy image showing hypometabolism in left temporal lobe. (a) Transaxial slice. (b) Coronal slice. (c) Temporal slice. (d) Surface-rendered images of the statistical analysis (3D-SSP), showing significant areas of reduced uptake. This is a z-score map normalised using the global mean with a threshold of $z > 2$ and overlaid on the patient MRI. This clearly identifies reduced metabolic activity in the left temporal lobe (Cortex ID, GE Healthcare)

step to previous images for longitudinal evaluation or to other modalities for visualisation and display, a co-registration step to standard anatomical templates for statistical comparisons against normal patient databases and univariate or multivariate statistical analysis tools for this purpose, including some kind of intensity normalisation step to account for differences in global measured activity between patients. Statistical comparisons can be done using regions of interest (ROI) or on a voxel-by-voxel basis. Most use simple t-tests or a number of standard deviations to map abnormal regions (Scenium and Cortex ID); other more sophisticated methods use multivariate-type statistics to look at how well each individual patient's pattern fits to an expected pathological pattern [12], e.g., the pattern of regional cerebral glucose metabolism associated with Parkinson's disease.

Fig. 4.8 Diagram of AC-PC line for the standard and individual brain for anatomical localisation [16]



4.5.1 Anatomical Standardisation

In order to statistically compare patient images to a control database, the patient image is anatomically standardised, often referred to as spatial normalisation. There are a number of different image templates or brain atlases available [13] that are created from an average of a number of normal datasets such as the Montreal Neurological Institute (MNI) templates [14, 15]. Images are re-orientated, transformed and warped to map the patient image to the template image in standard space [13, 16]. Spatial coordinates x , y and z , with reference to the x -axis through the Anterior Commissure-Posterior Commissure (ac-pc) line (Fig. 4.8), can then be used to anatomically localise abnormalities in the PET images [13, 17].

4.5.2 Intensity Normalisation

Once the patient study has been mapped to standard space, in order to perform a comparison with metabolic FDG uptake, the dataset must also be normalised for the relative intensity. This is to account for non-pathological differences in uptake for intra-subject comparison and between the patient study and the control database due to differences in imaging protocol, such as differences in administered activity. There are a number of options for intensity normalisation. One option is to simply take the total global counts and normalise to the cerebral global mean. However this can introduce bias if there are large outliers that skew the mean value. To avoid this sort of phenomenon, a reference region can be chosen that is known to be less affected by the disease process; cerebellum, thalamus or pons are popular choices depending on the indication. For example, it is common to use the cerebellum for both differential diagnosis of Alzheimer's disease or for seizure focus localisation in epilepsy. For others, it can be difficult to find an unaffected region. Data-driven intensity normalisation techniques for PET images have also been used to overcome these issues [18].

Figure 4.9 shows an example of statistical analysis for a ^{18}F -FDG scan for a pre-surgical epilepsy patient using Cortex ID. All four images show the same patient

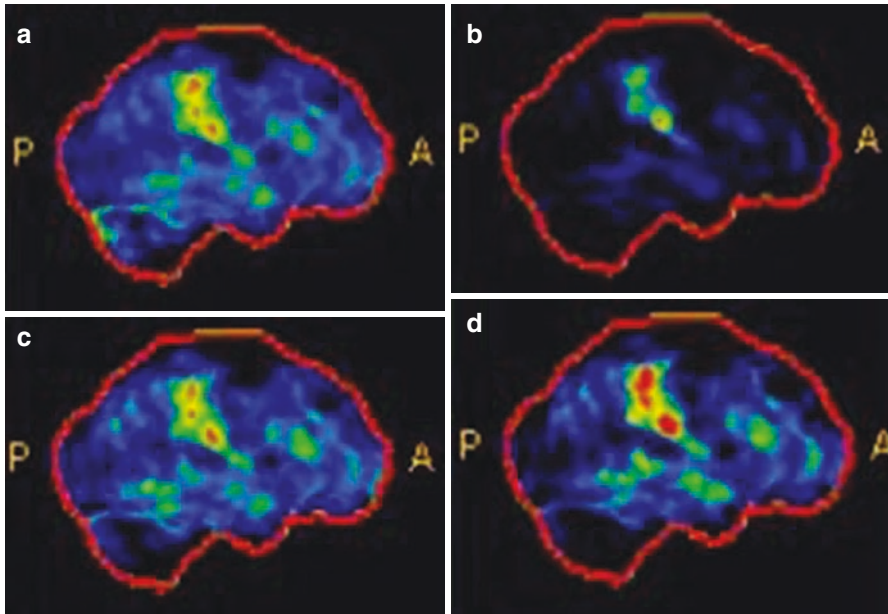


Fig. 4.9 Example patient statistical surface projections, showing effects of intensity normalisation method, processed on commercial software (Cortex ID, GE Healthcare). (a) Cerebellum. (b) Thalamus. (c) Pons. (d) Global mean

with different normalisations, (a) cerebellum, (b) thalamus, (c) pons and (d) global cortical mean), illustrating how the chosen normalisation method can affect the results.

4.5.3 Statistical Analysis

The same statistical analysis methods can be used to statistically evaluate ROI-based data as well as voxel-wise data. In this chapter we will use voxel-by-voxel data to describe the method, but ROI could be substituted. Now that the individual patient data has been spatially normalised and intensity normalised a statistical analysis that compares this patient's image to the normal database, image can be performed at each voxel. For example, a z -score can be calculated where z is the number of standard deviations of the patient's voxel value away from the mean voxel value in the normal database. It is important that the age range of individuals that make up the normal database should not be significantly different from that of the patient, as there are known to be systematic differences in cortical glucose metabolism with respect to age [19]. A z -score map can then be displayed onto a corresponding anatomical image or onto a cortical surface rendering where $z < 0$ shows hypermetabolism and $z > 0$ shows hypometabolism (Figs. 4.5d and 4.7d). This allows a threshold to be set to show only the voxels above this threshold (typically $z \sim 2$ corresponding to a p value of 0.05) on a surface rendered image.

4.5.4 Limitations

There are limitations to voxel-based statistical analysis which users should be aware of when reporting. Transformation errors can occur when mapping an individual's unique anatomical variations on to the template used to create the standard space. This may lead to incorrect deformations and incorrect mapping of brain structures. Spatial smoothing can ameliorate this effect to some extent, but if the anatomical deviation is, for example, unusual brain anatomy, atrophy, surgical resection or of a different age to the template used, then gross mismatches can occur. For paediatric populations cortical gyral folding is age dependent and has been shown not to map to adult MNI standard space terribly well [20] and the normal cortical glucose metabolic rate in children under the age of 10 can be distinctly different to that of adults [21, 22]. In this case it is more appropriate to use an age-matched paediatric population [23], and some commercial applications allow the employment of a locally developed database to be used in their pipelines [24]. In conclusion while these automated image analysis pipelines can be useful, the user must be well informed in normal neuroanatomy and physiology as well as the statistical theory used to calculate these visualisation aids.

Key Points

- Caffeine, alcohol or drugs that may affect cerebral glucose metabolism must be avoided for patient preparation and during the fasting period for the scan. Patients are required to stay in a quiet and dimly lit room for several minutes prior to injection and during the uptake phase to avoid enhanced uptake due to brain activity typically in the visual and/or auditory cortex.
- Once sufficient uptake time has passed (30–60 min), the patient should be carefully positioned, aligning the orbital-meatal plane in the x-axis and median sagittal plane in the y-axis. Scan time is dependent on scanner sensitivity and local protocol. To improve image quality attenuation maps can be created to provide attenuation correction and dynamic imaging can provide benefits to account for patient movement. Once reconstructed, it is important to ensure that the images are correctly displayed in a standard and symmetrical anatomical position in order to ensure consistent reporting and avoid potential artefacts in the image (for example in reporting interictal epilepsy an incorrect reconstruction may cause asymmetries in the uptake pattern in the temporal lobes wrongly indicative of seizure focus).
- There are a variety of PET analysis methods to quantify functional information related to neurodegenerative disease. These software packages can realign images to previous images for longitudinal evaluation or to other modalities for visualisation and display and can perform co-registration to standard anatomical templates for statistical comparisons against normal patient databases.

References

1. Purandare NC, Puranik A, Shah S. Common malignant brain tumors: can ¹⁸F-FDG PET/CT aid in differentiation? *Nucl Med Commun.* 2017;38(12):1109–16.
2. Demetriades AK, Almeida AC, Bhargoo RS, Barrington SF. Applications of positron emission tomography in neuro-oncology: a clinical approach. *Surgeon.* 2014;12(3):148–57. <https://doi.org/10.1016/j.surge.2013.12.001>. Epub 2014 Mar 11
3. Varrone A, Asenbaum S, Borghat TV, Booij J, Nobili F, Nagren K, et al. EANM procedure guidelines for PET brain imaging using [¹⁸F]FDG, version 2. *Eur J Nucl Med Mol Imaging.* 2009;36(12):2103–10.
4. Waxman AD, Herholz K, Lewis DH, Herscovitch P, Minoshima S, Ichise M, et al. Society of nuclear medicine procedure guideline for FDG PET brain imaging. v1. Society of nuclear medicine molecular imaging. 2009.
5. Sarikaya I. PET studies in epilepsy. *Am J Nucl Med Mol Imaging.* 2015;5(5):416–30.
6. Boellaard R, O'Doherty MJ, Weber WA, Mottaghy FM, Lonsdale MN, Stroobants SG, et al. FDG PET and PET/CT: EANM procedure guidelines for tumour PET imaging. v1. *Eur J Nucl Med Mol Imaging.* 2010;37(1):181–200.
7. Leiderman DB, Albert P. The dynamics of metabolic change following seizures as measured by positron emission tomography with fludeoxyglucose F 18. *Arch Neurol.* 1994;51(9):932–6.
8. Administration of Radioactive Substances Advisory Committee. Notes for guidance on the clinical administration of radiopharmaceuticals and use of sealed radioactive sources. UK: Public Health England; March 2018.
9. Lassmann M, Biassoni L, Monsieurs M, Franzius C, EANM Dosimetry and Paediatrics Committees. The new EANM paediatric dosage card: additional notes with respect to F-18. *Eur J Nucl Med Mol Imaging.* 2008;35(9):1666–8.
10. Tong S, Alessio AM, Kinahan PE. Image reconstruction for PET/CT scanners: past achievements and future challenges. *Imaging Med.* 2010;2(5):529–45.
11. Dickson JC, O'Meara C, Barnes A. A comparison of CT- and MR-based attenuation correction in neurological PET. *Eur J Nucl Med Mol Imaging.* 2014;41(6):1176–89.
12. Spetsieris PG, Ma Y, Dhawan V, Eidelberg D. Differential diagnosis of parkinsonian syndromes using PCA-based functional imaging features. *NeuroImage.* 2009;45(4):1241–52.
13. Manda PK, Mahajan R, Dinovic ID. Structural brain atlases: design, rationale, and applications in normal and pathological cohorts. *J Alzheimers Dis.* 2012;31:169–88.
14. Brett M, Johnsrude IS, Owen AM. The problem of functional localization in the human brain. *Nat Rev Neurosci.* 2002;3:243–9.
15. Mazziotta JC, Toga AW. A probabilistic atlas of the human brain: theory and rationale for its development: the international consortium for brain mapping (ICBM). *NeuroImage.* 1995;2:89–101.
16. Minoshima S, Koeppe RA, Frey KA, Kuhl DE. Anatomic standardization: linear scaling and nonlinear warping of functional brain images. *J Nucl Med.* 1994;35(9):1528–37.
17. Minoshima S, Kuhl DE, Foster NL, Koeppe RA, Frey KA. A diagnostic approach in alzheimer's disease using three-dimensional stereotactic surface projections of fluorine-18-FDG PET. *J Nucl Med.* 1995;36(7):1238–48.
18. Borghammer P, Aanerud J, Gjedde A. Data-driven intensity normalization of PET group comparison studies is superior to global mean normalization. *NeuroImage.* 2009;46(4):981–8.
19. Shen X, Liu H, Hu H, Shi P. The relationship between cerebral glucose metabolism and age: report of a large brain PET data set. *PLoS One.* 2012;7(12):e51517.
20. Groeschel S, Vollmer B, King M, Connelly A. Developmental changes in cerebral grey and white matter volume from infancy to adulthood. *Int J Dev Neurosci.* 2010;28(6):481–9.
21. Van Bogaert P, Wikler D, Damhaut P, Szliwowski H, Goldman S. Regional changes in glucose metabolism during brain development from the age of 6 years. *NeuroImage.* 1998;8(1):62–8.

22. Kinnala A, Suhonen-Polvi H, Aärimaa T, Kero P, Korvenranta H, Ruotsalainen U, et al. Cerebral metabolic rate for glucose during the first six months of life: an FDG positron emission tomography study. *Arch Dis Child Fetal Neonatal Ed.* 1996;74(3):153–7.
23. De Blasi B, Barnes A, Galazzo IB, Hua C, Shulkin B, Koepp M, et al. Age-specific ^{18}F -FDG image processing pipelines and analysis are essential for individual mapping of seizure foci in paediatric patients with intractable epilepsy. *J Nucl Med.* 2018; <https://doi.org/10.2967/jnumed.117.203950>.
24. Schenk V. Scenium v.1 and PET, white paper paper. USA: Siemens, Medical Solutions; 2006.